

## Synthesis and Memory Device Characteristics of New Sulfur Donor Containing Polyimides

Nam-Ho You,<sup>†,‡</sup> Chu-Chen Chueh,<sup>†,‡</sup> Cheng-Liang Liu,<sup>‡</sup> Mitsuru Ueda,<sup>\*,†</sup> and Wen-Chang Chen<sup>\*,†,§</sup>

<sup>†</sup>Department of Organic and Polymeric Materials, Tokyo Institute of Technology, 2-12-1 Ookayama, Meguro-ku, Tokyo 152-8552, Japan, <sup>‡</sup>Department of Chemical Engineering, National Taiwan University, Taipei, Taiwan 106, and <sup>§</sup>Institute of Polymer Science and Engineering, National Taiwan University, Taipei, Taiwan 106

Received March 7, 2009; Revised Manuscript Received May 4, 2009

**ABSTRACT:** The synthesis and memory device characteristics of two new poly[2,7-bis(phenylenesulfanyl)thianthrene–hexafluoroisopropylidenedipthalimide] (APTT-6FDA) and poly[4,4'-thiobis(*p*-phenylenesulfanyl)–hexafluoroisopropylidenedipthalimide] (3SDA-6FDA) are reported. The sulfur-containing APTT and 3SDA as electron donor were designed to enhance electron-donating and charge-transporting characteristics for the device application. The optical band gaps of APTT-6FDA and 3SDA-6FDA estimated from the absorption edges were 3.51 and 3.46 eV, which probably resulted from the difference in the structural coplanarity. The estimated energy levels (HOMO, LUMO) of APTT-6FDA and 3SDA-6FDA were (–5.55, –2.04) and (–5.71, –2.25) eV, respectively. The memory device with the configuration of ITO/polymers/Al showed nonvolatile memory characteristics with the low turn-on threshold voltages of 1.5 V (APTT-6FDA) and 2.5 V (3SDA-6FDA), probably resulting from the difference in the HOMO energy level. Also, the memory devices could be repeatedly written, read, and erased. The on/off current ratios of the devices were all around 10<sup>4</sup> in ambient atmosphere. The relatively higher dipole moments of the sulfur-containing polyimides compared to the triphenylamine-based polyimide provided a stable CT complex for the flash memory device. The above electronic properties were further confirmed by the density functional theory (DFT) method at the B3LYP level with the 6-31G(d) basis set. The present study suggested that the new sulfur-containing polyimides would have potential applications for memory devices.

### Introduction

Polymer-based memory devices have attracted significant scientific interest recently due to the advantages of rich structure flexibility, low cost, solution processability, and three-dimensional stacking capability.<sup>1,2</sup> The studied polymer systems basically consist of different ratios between electronic donor and acceptor, including conjugated polymers,<sup>3–5</sup> electron donor/acceptor polymers,<sup>6–9</sup> polymer/organic molecule blends,<sup>10,11</sup> polymer/metal hybrid materials,<sup>12–15</sup> polymer/metal complex,<sup>16</sup> and others.<sup>17–19</sup> Different kinds of memory devices have been also discovered, such as dynamic random access memory (DRAM), write-once-read-many (WORM), and flash memory, etc. The driving force behind these memory devices basically depends on the “trapping–detrapping”, “charge transfer”, “conformational change”, and “nanocomposite redox”, as summarized by Kang and co-workers.<sup>1</sup>

Among the studied polymer systems, polyimides are promising materials for device applications due to their excellent physical and chemical properties besides the irreplaceable switching property.<sup>1</sup> Kang and co-workers reported the TP6F-PI consisted of triphenylamine (electron donor) and hexafluoroisopropyl bis(phthalic dianhydride) (6FDA, electron acceptor), which exhibited the DRAM characteristic.<sup>7</sup> Later, they also developed various kinds of electron donor and acceptor containing polyimides for the memory device applications. Otherwise, Ree and co-workers reported novel nonvolatile memory device from

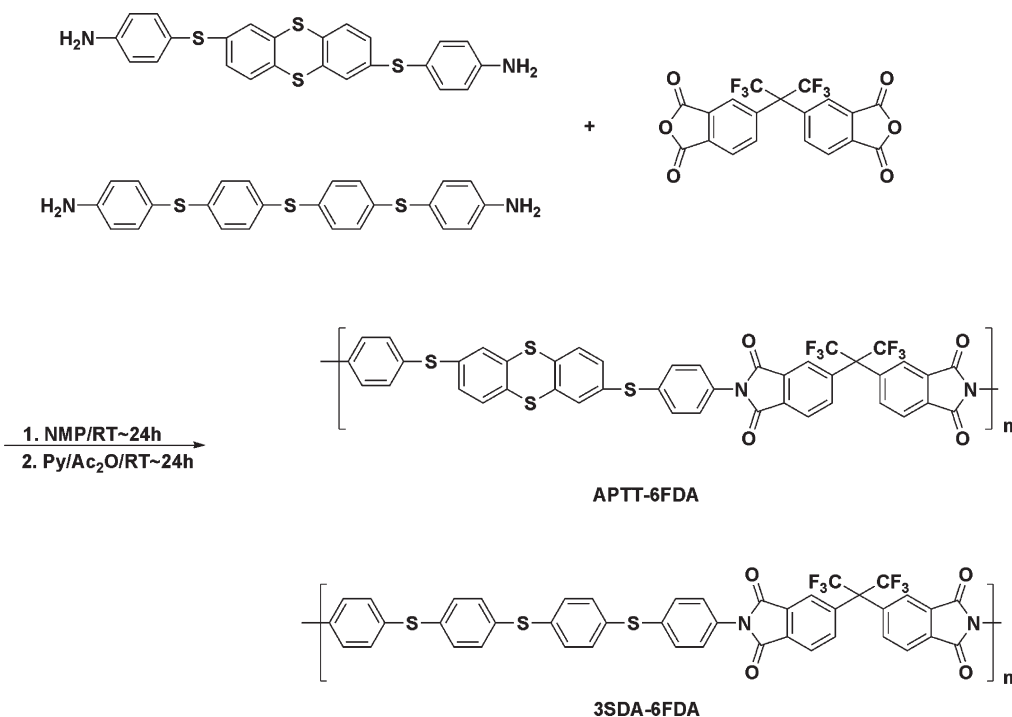
polyimide consisting of 6FDA (main chain) and carbazole (side chain), which exhibited a relatively high on/off ratio and long-term stability.<sup>8</sup> Although various polyimide-based memory devices have been developed, sulfur-containing polyimides on such applications have not been explored yet. The electron-rich sulfur-containing polymers could be easily oxidized and serve as a good candidate as electron donor. In fact, Janietz et al. reported that polyimides containing thianthrene units had a low oxidation peak  $E_{ox}$  at 1.5 V.<sup>20</sup> Moreover, polymers and organic materials containing sulfur atoms have been well studied for device application such as light-emitting diodes (OLEDs), charge transfer (CT) complex, and thin-film transistor (TFTs).<sup>21,22</sup> Recently, we have developed various sulfur-containing polyimides with the characteristics of high refractive index, good transparency, and low birefringence but also excellent thermal stability.<sup>23–26</sup> The electron-rich sulfur-containing groups generally have high dipole moments as well as good electron-donating and charge-transporting characteristics. Such characteristics may lead to stable high-performance memory devices. Thus, it would be of interest to explore new sulfur-containing polyimides for memory device applications.

In this paper, we report the synthesis and memory device characteristics of two new poly[2,7-bis(phenylenesulfanyl)thianthrene–hexafluoroisopropylidenedipthalimide] (APTT-6FDA) and poly[4,4'-thiobis(*p*-phenylenesulfanyl)–hexafluoroisopropylidenedipthalimide] (3SDA-6FDA). These new polyimides were synthesized by a two-step polycondensation of 2,7-bis(4-aminophenylenesulfanyl)thianthrene (APTT) and 4,4'-thiobis[(*p*-phenylenesulfanyl)aniline] (3SDA) with 6FDA via the poly(amic acid) (PAA) solution, followed by chemical imidization

<sup>†</sup> These authors contributed equally to this work.

\*To whom all correspondence should be addressed. E-mail: ueda.m.ad@m.titech.ac.jp (M.U.); chenwc@ntu.edu.tw (W.-C.C.).

Scheme 1. Synthesis of the Studied Polyimides APTT-6FDA and 3SDA-6FDA



using pyridine and acetic anhydride, as shown in Scheme 1. The use of APTT and 3SDA as electron donors as expected to enhance electron-donating and charge-transporting capacity with 6FDA for the device application. The thermal, optical, and electrochemical properties of the APTT-6FDA and 3SDA-6FDA were characterized. The memory behavior was conducted by a simple sandwich device configuration consisted of spin-coated polymer films between indium–tin oxide (ITO) bottom electrode and Al top electrode. Density functional theory (DFT) method at the B3LYP level with the 6-31G(d) basic set was used to analyze the geometry and electronic properties of the studied polymers. The obtained electrical characteristics suggest that APTT-6FDA and 3SDA-6FDA are good candidates for non-volatile flash type memory.

## Experimental Section

**Materials.** *p*-Fluorothiophenol and *p*-aminothiophenol were purchased from TCI, Japan. Fuming sulfuric acid (30% oleum) was obtained from Wako, Japan. *N,N*-Dimethylformamide (DMF) and *N*-methyl-2-pyrrolidone dehydrated (NMP) were obtained from Wako, Japan, and used as received. 6FDA (from TCI, 99%) was recrystallized from acetic anhydride and dried at 100 °C under vacuum before used for polymerization. APTT and 3SDA were prepared according to our previous report.<sup>24,26</sup>

**Synthesis of Poly[2,7-bis(phenylenesulfanyl)thianthrene–hexafluoroisopropylidenediphthalimide] (APTT-6FDA).** 6FDA (0.4443 g, 1.00 mmol) was added into a solution of APTT (0.4627 g, 1.00 mmol) in dehydrated NMP (solid contents 15%) under a nitrogen atmosphere. The reaction mixture was stirred at room temperature for 24 h to give a PAA solution. A reaction mixture of acetic anhydrides (0.1479 g, 1.49 mmol) and pyridine (0.1146 g, 1.49 mmol) was added to the above PAA solution. The reaction mixture was stirred at room temperature under a nitrogen atmosphere for 24 h. The resulting mixture was poured into methanol, and the precipitate was collected by filtration and washed with methanol. The final product was dried at 100 °C under vacuum for 5 h, and the polymer yield was 92%. The number-average molecular weights ( $M_n$ ) and weight-average molecular weight ( $M_w$ ) estimated from gel permeation

chromatography (GPC) were  $1.31 \times 10^5$  and  $3.23 \times 10^5$  Da, respectively, with the polydispersity index ( $PDI = M_w/M_n$ ) was 2.47. <sup>1</sup>H NMR (300 MHz, CDCl<sub>3</sub>-d<sub>6</sub>, ppm): 8.03 (d, 2H), 7.91 (s, 2H), 7.87 (d, 2H), 7.51 (s, 2H), 7.42–7.34 (m, 10H), 7.28 (d, 2H). FT-IR (KBr, cm<sup>-1</sup>): ~1783 (asym, C=O), ~1728 (sym, C=O), 1495 (–C–C–), 1372 (C–N), and 1233 cm<sup>-1</sup> (C–S). Anal. Calcd for C<sub>43</sub>H<sub>21</sub>F<sub>6</sub>N<sub>2</sub>O<sub>4</sub>S<sub>4</sub> (wt %): C, 59.23; H, 2.43; N, 3.21. Found: C, 58.82; H, 2.67; N, 2.99.

**Synthesis of Poly[4,4'-Thiobis(*p*-phenylenesulfanyl)–hexafluoroisopropylidenediphthalimide] (3SDA-6FDA).** This polyimide was prepared by a similar procedure according to synthesis of APTT-6FDA. Yield: 98%. The number-average molecular weights ( $M_n$ ) and weight-average molecular weight ( $M_w$ ) estimated from gel permeation chromatography (GPC) were  $7.06 \times 10^4$  and  $9.74 \times 10^4$  Da, respectively, with the polydispersity index ( $PDI = M_w/M_n$ ) was 1.38. <sup>1</sup>H NMR (300 MHz, CDCl<sub>3</sub>-d<sub>6</sub>, ppm): 8.02 (d, 2H), 7.92 (s, 2H), 7.86 (d, 2H), 7.44–7.28 (m, 16H). Anal. Calcd for C<sub>43</sub>H<sub>24</sub>F<sub>6</sub>N<sub>2</sub>O<sub>4</sub>S<sub>3</sub> (wt %): C, 61.18; H, 2.86; N, 3.34. Found: C, 61.28; H, 2.87; N, 3.32.

**Characterization of Polyimides (PIs).** The FT-IR spectra of APTT-6FDA and 3SDA-6FDA on a KBr substrate were acquired using a Horiba FT-120 Fourier transform spectrophotometer. The <sup>1</sup>H NMR spectrum was recorded on a Bruker DPX-300S spectrometer at the resonant frequencies of 300 MHz using CDCl<sub>3</sub>-d<sub>6</sub> and DMSO-*d*<sub>6</sub> as the solvent. Elemental analyses were performed on a Yanaco MT-6 CHN recorder elemental analysis instrument. Thermogravimetric analysis (TGA) was performed on a Seiko TG/DTA 6300 under a nitrogen atmosphere at a heating rate of 10 °C/min. Differential scanning calorimetry (DSC) was obtained using a Seiko DSC 6300 at a heating rate of 10 °C/min. Ultraviolet–visible (UV–vis) absorption spectra were recorded on a Hitachi U-4100 spectrophotometer. For the thin film spectra, polymers were first dissolved in tetrahydrofuran (10 mg/mL) and filtered through 0.45 μm pore size of PTFE membrane syringe filters, spin-coated at a speed rate of 1000 rpm for 60 s onto fused silica. Cyclic voltammetry was performed at room temperature using a working electrode (ITO, polymer films area about 0.5 × 0.7 cm<sup>2</sup>), a homemade reference electrode Ag/AgCl, and a counter electrode (Pt wire) at a sweeping rate of 0.1 V/s (CHI 611B electrochemical analyzer). A 0.1 M solution of tetrabutylammonium perchlorate (TBAP)

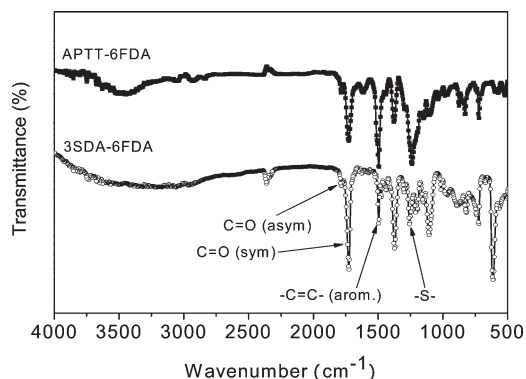


**Figure 1.** FTIR spectra of APTT-6FDA and 3SDA-6FDA.

in anhydrous acetonitrile was used as an electrolyte. The energy level of the HOMO was determined from the onset oxidation ( $E_{\text{onset}}^{\text{ox}}$ ) based on the reference energy level of ferrocene (4.8 V below the vacuum level) according to the following relation:  $\text{HOMO} = -e(E_{\text{onset}}^{\text{ox}} - E_{\text{ferrocene}}^{1/2} + 4.8) \text{ eV}$ . The LUMO level was calculated from the HOMO and the value of optical band gap according to the relation  $\text{LUMO} = \text{HOMO} + E_{\text{g}}^{\text{opt}} \text{ (eV)}$ .<sup>27</sup> The thickness of polymer films was measured with an Alpha-step 500 surface profiler (TENCOR). Atomic force micrographs (AFM) of the polymer films on the device surface were obtained with a Nanoscope 3D Controller AFM (Digital Instruments, Santa Barbara, CA) operated in the tapping mode at room temperature. Commercial silicon cantilevers (Nanosensors, Germany) with typical spring constants 21–78 N m<sup>-1</sup> was used, and the images were taken continuously with the scan rate of 1.0 Hz.

**Fabrication and Measurement of the Memory Device.** The memory device was fabricated on the indium–tin oxide (ITO)-coated glass, with the configuration of ITO/polymer/Al. Before the fabrication of the polymer layer, the glass was precleaned by ultrasonication with water, acetone, and isopropanol each for 15 min. Afterward, 0.5 wt % of APTT-6FDA or 3SDA-6FDA polymer solution in tetrahydrofuran (THF) was first filtered through 0.45  $\mu\text{m}$  pore size of PTFE membrane syringe filter. Then, the filtered solution was spin-coated onto the precleaned ITO glass at a speed rate of 2000 rpm for 60 s and baked at 100 °C for 3 h under vacuum. The polymer film thickness was around 120–150 nm. The top metal electrode was obtained by a 300 nm Al through a shadow mask, and the active area of the device was 0.36 mm<sup>2</sup>. The current–voltage ( $I$ – $V$ ) characteristics and the write–read–erase–reread cycles were performed using a Keithley 4200 semiconductor parametric analyzer. All of the electronic measurements were performed in ambient atmosphere.

**Theoretical Analysis.** Molecular calculations studied in this work have been performed with Gaussian 03 program package.<sup>28</sup> The ground state geometry and electronic structures of the basic unit of APTT-6FDA and 3SDA-6FDA were optimized by means of the density functional theory (DFT) method at the B3LYP level of theory (Beckes-style three-parameter density functional theory using the Lee–Yang–Parr correlation functional) with the 6-31G(d) basic set.

## Results and Discussion

**Polymer Characterization.** Figures 1 and 2 show the FT-IR and <sup>1</sup>H NMR spectra of the prepared polyimides, APTT-6FDA and 3SDA-6FDA, respectively. In the FT-IR spectra, the characteristic peaks at 1783, 1780 (asym, C=O), 1728, 1721 (sym, C=O), and 1372, 1369 cm<sup>-1</sup> (C–N) are attributed to the imide group, indicating the complete imidization. Besides, the peak positions in the <sup>1</sup>H NMR spectra of APTT-6FDA and 3SDA-6FDA are also consistent with the proposed structures. Figure 3 displays the two-dimensional

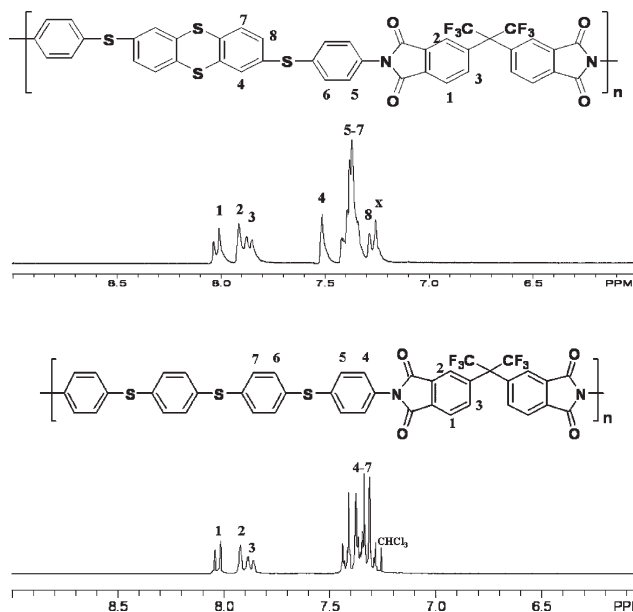


**Figure 2.** <sup>1</sup>H NMR spectra of APTT-6FDA and 3SDA-6FDA in CDCl<sub>3</sub> and DMSO, respectively.

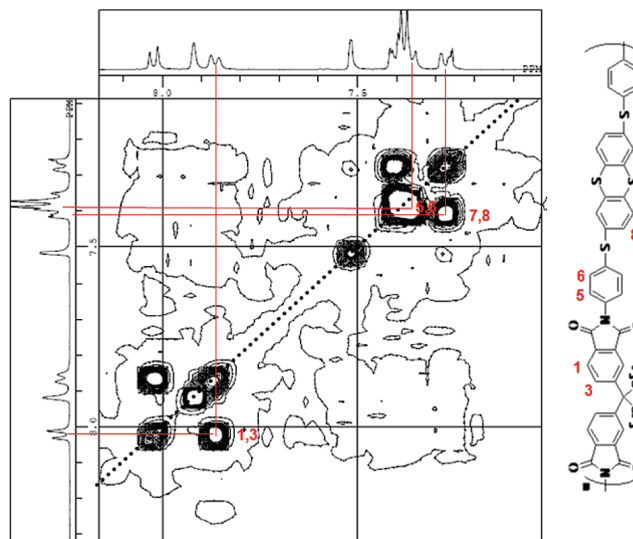


**Figure 3.** Two-dimensional H–H COSY NMR spectrum of APTT-6FDA in CDCl<sub>3</sub>.

H–H COSY NMR spectrum of the APTT-6FDA in CDCl<sub>3</sub>. The aromatic signals at 8.03 and 7.87 ppm are connected with each other, and these signals can be assigned to the aromatic protons at 1 and 3. Furthermore, the aromatic protons (7 and 8) adjacent to thioether units would be appeared the most upfield, and the strong correlation between these protons are observed at 7.35 and 7.28 ppm. Further spectra evidence for the proposed structure of the polymer was provided by <sup>13</sup>C NMR and Dept 135 spectroscopies (see Supporting Information S1). The elemental analysis (EA) results of C, H, and N contents are in a fair agreement with the theoretical content. The FT-IR, NMR, and elemental analysis suggest the successful preparation of the target APTT-6FDA and 3SDA-6FDA.

The APTT-6FDA and 3SDA-6FDA show good solubility in common organic solvents, such as DMF, DMAc, NMP, and THF. Thus, optical quality thin films for the memory device application could be obtained by spin-coating. The thermal properties of the PIs were evaluated by TGA and



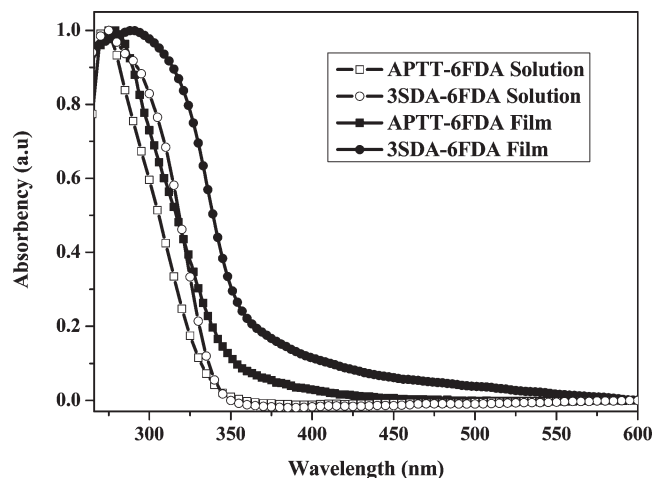


**Figure 4.** UV-vis absorption spectra of APTT-6FDA and 3SDA-6FDA on fused silica.

**Table 1.** Optoelectronic Properties and Calculated Energy Levels of the Studied Polymers

polymer	UV-vis, $\lambda_{\max}$ (nm)		$E_g$ (eV)		HOMO (eV)		LUMO (eV)	
	soln <sup>a</sup>	film	calc	exp <sup>b</sup>	calc	exp	calc	exp <sup>c</sup>
APTT-6FDA	275	280	3.05	3.51	-5.61	-5.55	-2.56	-2.04
3SDA-6FDA	276	290	2.96	3.46	-5.63	-5.71	-2.67	-2.25

<sup>a</sup>In THF dilute solution. <sup>b</sup>Estimated from the absorption edge of the film. <sup>c</sup>LUMO = HOMO +  $E_g^{\text{opt}}$  (eV).

DSC measurements, and the experimental curves are appended in the Supporting Information. The APTT-6FDA and 3SDA-6FDA not only showed excellent thermal stability with the 10% weight loss temperature ( $T_{10\%}$ ) at 541 and 539 °C but also possessed high glass transition temperatures of 272 and 246 °C, respectively.

**Optical and Electrochemical Properties.** Figure 4 depicts the UV-vis absorption spectra of the studied polymers in THF solution and thin film state, respectively. The obtained optical properties are summarized in Table 1. As shown in Figure 4, APTT-6FDA shows absorption maxima ( $\lambda_{\max}$ ) around 275 and 280 nm in solution and thin film state, while those of 3SDA-6FDA are around 276 and 290 nm, respectively. The estimated optical band gap ( $E_g^{\text{opt}}$ ) of APTT-6FDA and 3SDA-6FDA from the absorption edges of polymer thin films are about 3.51 and 3.46 eV, respectively. These results are similar to the values of their derivatives reported in our previous studies.<sup>24,26</sup> The larger  $\lambda_{\max}$  and smaller band gap of 3SDA-6FDA than APTT-6FDA probably resulted from the better coplanarity of the polymer structure, which will be discussed in the Theoretical Analysis section.

Figure 5 shows the cyclic voltammogram (CV) of APTT-6FDA and 3SDA-6FDA films on Pt electrode using a 0.1 M solution of tetrabutylammonium perchlorate (TBAP) in anhydrous acetonitrile electrolyte. All of the related electrochemical data are also listed in Table 1. The APTT-6FDA CV showed two oxidation peaks, but the 3SDA-6FDA CV exhibited only one oxidation peak. The two oxidation peaks of the APTT-6FDA could be due to the sulfur-containing ring and phenylene sulfur outside of the ring structure. The onset oxidation ( $E_{\text{onset}}^{\text{ox}}$ ) for APTT-6FDA and 3SDA-6FDA is around 1.19 and 1.35 V vs Ag/Ag<sup>+</sup>, and thus the estimated highest occupied molecular orbital (HOMO) level is -5.55 and -5.71 eV, respectively. Note that the  $E_{\text{ferrocene}}^{1/2}$  is 0.44 V from the CV measurement without any polymer film coated

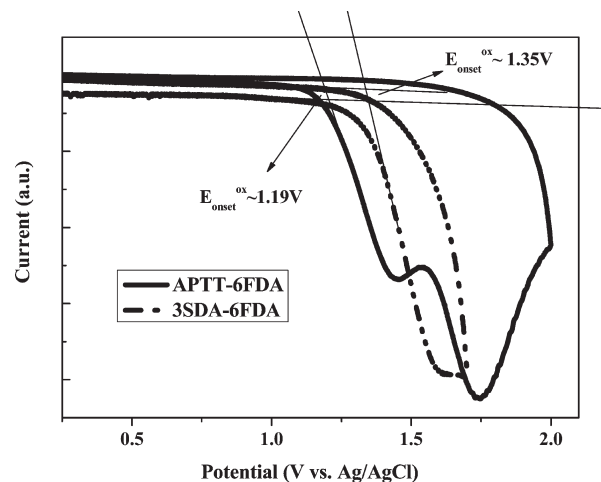


**Figure 5.** Cyclic voltammograms of APTT-6FDA and 3SDA-6FDA.

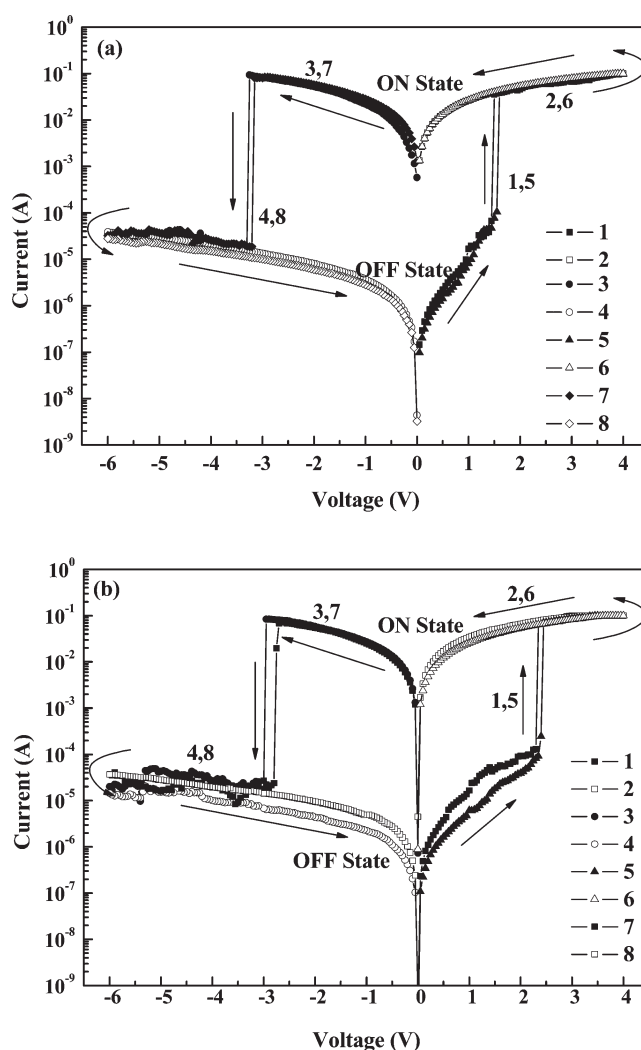


**Figure 6.** Current-voltage ( $I$ - $V$ ) characteristics of (a) APTT-6FDA and (b) 3SDA-6FDA.

on ITO glass. Besides, the lowest occupied molecular orbital (LUMO) energy level of APTT-6FDA and 3SDA-6FDA could be estimated from the difference between the optical band gap and HOMO energy, and the values are -2.04 and -2.25 eV. These results indicate that the 3SDA-based polymer structure rather than APTT-based one could provide a lower and more stable HOMO or LUMO energy level.

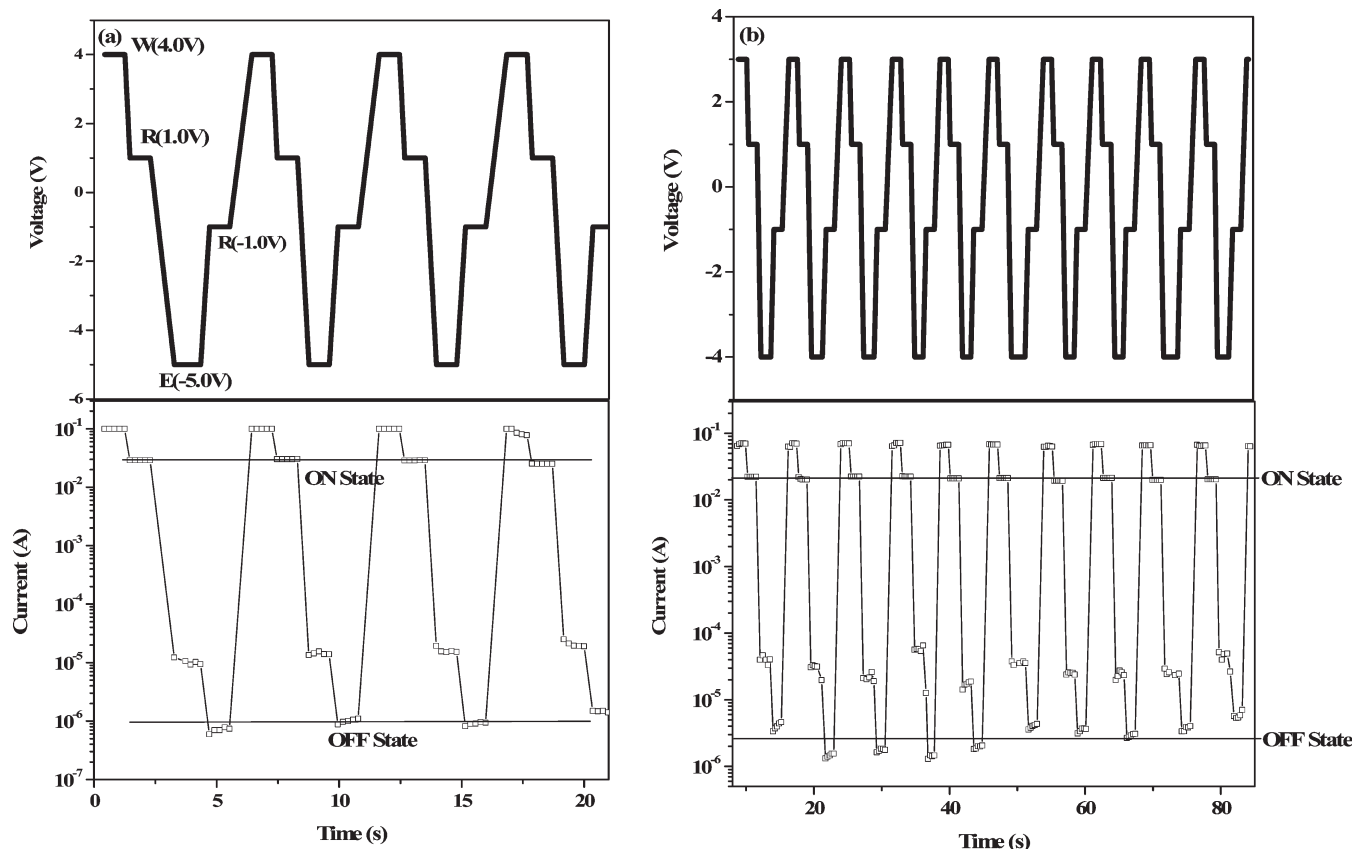


**Figure 7.** Applied voltage sequence and the typical current responses to WRER cycles of (a) APTT-6FDA and (b) 3SDA-6FDA.

**Memory Device Characteristics of the Polymers.** The memory behavior of APTT-6FDA and 3SDA-6FDA was tested by the  $I$ – $V$  characteristics of ITO/polymers/Al device. As reported in the literature, the polymer memory devices store data based on the high- and low-conductivity response to the applied voltages.<sup>1</sup> Figure 6 shows the typical  $I$ – $V$  curves of the polymer devices fabricated with APTT-6FDA and 3SDA-6FDA. Taking APTT-6FDA for example, as the initial voltage swept from 0 to 1.5 V, current is very low and in the order of  $10^{-7}$ – $10^{-4}$  A. It reveals that the device is in a low-conductivity state and assigned as OFF-state or “0” signal in data storage. However, the continuous sweeping voltage induces an abrupt increase in current around 1.5–1.6 V, which is defined as the switching threshold voltage. After switching, the current reaches at almost 3 orders of magnitude higher than that in a low-conductivity state. It indicates that the device is transformed from the low-conductivity state to a high-conductivity state and assigned as ON-state or “1” signal in data storage. This electronic transition from OFF-state to ON-state serves as the “writing” process. The device remains in a high conductivity (ON-state) during the subsequent second sweep from 4 to 0 V and does not relax to the OFF-state even after the power is turned off for 10 min. This distinct bielectrical state in the voltage range of 0–1.6 V allows a voltage (e.g., 1.0 V) to read the OFF signal (before writing) and ON signal (after writing) of the memory. As the voltage sweeps negatively from 0 to –6 V, an abrupt decrease in current is observed at a threshold voltage of about –3.2 V, corresponding to the “erasing” process for the memory device. Similarly, the device remains in a low conductivity (OFF-state) during the subsequent fourth sweep from –6 to 0 V and even after the power is turned off. The OFF-state can be further turned on to the ON-state and turned off back to the OFF-state by reapplying the switching threshold

voltages, as the fifth to the eighth sweep shown in Figure 6. Therefore, this memory device could be used as a flash type memory. However, as compared to APTT-6FDA, 3SDA-6FDA shows a much higher turn on threshold voltage of 2.5–2.6 V while the turn-off threshold voltage is only with a slight decrease. The increase in turn-on threshold voltage is obviously due to the lower HOMO energy level of 3SDA-6FDA than APTT-6FDA, which would provide a more stable CT complex as the case reported for PP6F–PI and TP6F–PI.<sup>1,7</sup> Note that the small surface roughness in the AFM images of the prepared polymer films suggests the good quality films (Figure S5), and thus the above memory characteristics are mostly resulted from the chemical structural effects. The simple write–read–erase–reread cycle for the polymer devices were also conducted, as shown in Figure 7. For both polymers, the duration of each sequential voltage pulse was 6 s, and the currents with the absolute value were measured for 5 points within each voltage impulse. Here, the write, read, erase, and reread (WRER) voltages were set to the switch-ON voltage, the read-ON voltage, the switch-OFF voltage, and the read-OFF voltage, respectively. For APTT-6FDA, the pulse voltages were set to W (4.0 V)–R (1.0 V)–E (–5.0 V)–R (–1.0 V) as shown in Figure 7a, and those of 3SDA-6FDA are in Figure 7b. The responding ON- and OFF-current demonstrates the memory behavior of these two polymers. Figure 8 shows the retention times and stress tests of both the ON and OFF states of APTT-6FDA and 3SDA-6FDA. No obvious degradation in current is observed for both ON- and OFF-state during the readout test. It indicated that the formed CT complex possessed a good stability. Moreover, the on/off ratios all kept around  $10^4$  throughout the measurement, and these ratios could also be confirmed in Figure 7.

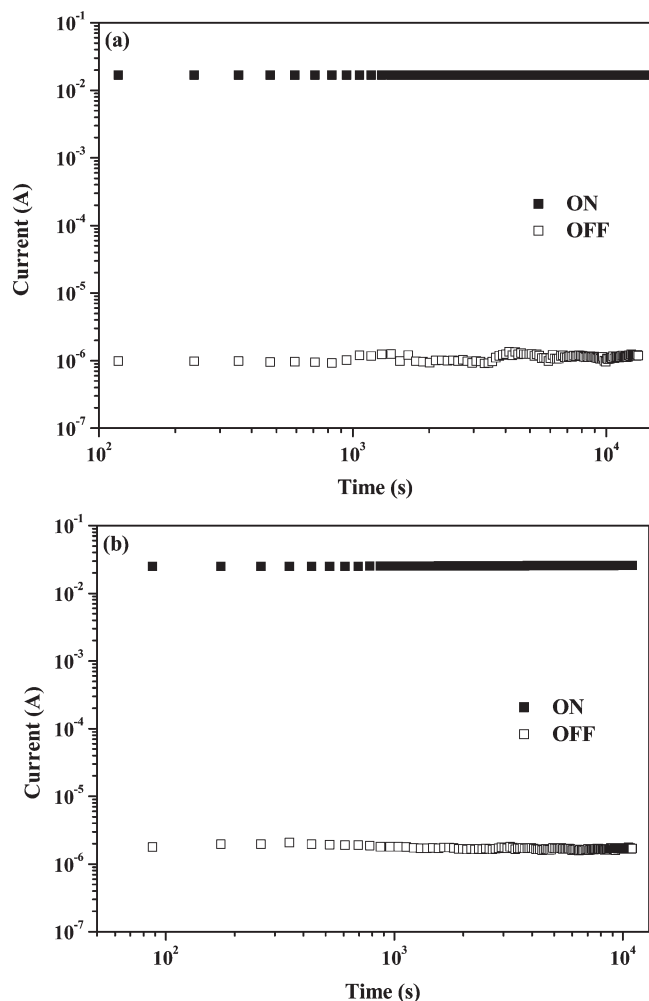


**Figure 8.** Stability of APTTITO/polymer/Al device resistance on continuous readout voltage: (a) APTT-6FDA (b) 3SDA-6FDA.

The above flash type memory behavior of the APTT-6FDA and 3SDA-6FDA devices was closer to the reported polyimide derivative, TP6F-PI and PP6F-PI.<sup>1,7</sup> However, it was different from the unipolar switching behavior induced by filament formation of 6F-HAB-PI<sup>8</sup> derivatives, and the discrepancy might arise from the disparate polymer structures, where the different pendants served as donor and attached to the main chain. The mechanism of the APTT-6FDA and 3SDA-6FDA memory behavior is believed to be similar to the photoinduced electron transfer mechanism observed in many photoconductive PI system.<sup>29–32</sup> It arises from the polarized charge transfer (CT) state between APTT/3SDA and 6FDA moieties under an applied field. Under an applied field, the dipole moment of exciton changes and leads to a splitting of the original exciton states.<sup>32</sup> In order to further clarify the memory mechanism of these new sulfur-containing polyimides, the theoretical analyses were explored (discussed in next section), and the reported TP6F-PI and PP6F-PI were taken for comparison.<sup>1,7</sup> The higher theoretical dipole moments of the APTT-6FDA and 3SDA-6FDA than that of TP6F-PI provide a more stable CT complex in comparison with TP6F-PI.<sup>1,7</sup> And so even after the driving power is turned off, the ON-state of the polymer devices could still remain as the behavior of PP6F-PI,<sup>1</sup> but the ON-state of TP6F-PI<sup>7</sup> returned to the OFF-state. However, different from PP6F-PI,<sup>1</sup> a reverse bias of about  $-2.8$  to  $-3.2$  V applied to APTT-6FDA or 3SDA-6FDA could dissociate the CT complex and

returns to the OFF-state. Its switch-off behavior is much like volatile TP6F-PI<sup>7</sup> instead. This result indicates that the polymer device based on these new sulfur-containing polyimides can be easily on and off by the voltage control. This nonvolatile-like memory behavior was also observed for the PAE system.<sup>9</sup> Furthermore, even though APTT-6FDA and 3SDA-6FDA possess low HOMO energy levels, the turn-on threshold voltages are still low, around  $1.5$ – $2.5$  V, as compared to that of PP6F-PI.<sup>1</sup> The low turn-on voltages is believed to be related to the electron-rich sulfur-containing polymer structures, which may provide a larger dipole moment as evidenced in the theoretical analysis below. The above result suggests that these new sulfur-containing polyimides have potential applications for memory devices. Also, the memory properties could be further tuned by incorporating different sulfur-containing moiety into polyimide.

**Theoretical Study on Geometry and Electronic Properties.** Molecular simulation on the basic unit of APTT-6FDA and 3SDA-6FDA was carried out by DFT//B3LYP/6-31G(d). The sketch map of the structures for the basic unit of APTT-6FDA and 3SDA-6FDA (APTT or 3SDA as electron donor and phthalimide as electron acceptor, respectively) and optimized structures are plotted in the left of Figure 9a and 9b, respectively. Presumably, the DFT calculations for the thianthrene unit provide the reliable bond length as evidence by the X-ray results.<sup>33</sup> The theoretical packing angle for thianthrene is  $136.50^\circ$ , which is in a good agreement with the experimental result of  $128.09^\circ$ .<sup>33</sup> Besides, the noncoplanar geometry is shown between the sulfur-substituted phenylene and thianthrene unit. Both these two factors contribute to the twist conformation of APTT-6FDA. The DFT optimized geometries of 3SDA are also in excellent agreement with data obtained from X-ray analyses of 4,4'-bis[(phenyl-sulfonyl)methyl]biphenyl.<sup>34</sup> The better coplanarity of the 3SDA-6FDA than that of APTT-6FDA could be due to the structure difference on the sulfur-containing moiety. In the APTT moiety, sulfur-substituted phenylene and thianthrene are linked at the two different meta-positions, but those of the 3SDA are on the para-linkage. The standard deviations for C–S bond length ( $1.794$  Å, theoretical calculation;  $1.768$  Å, experimental data) and dihedral angle ( $67.88^\circ$ , theoretical calculation;  $64.20^\circ$ , experimental data) between the two adjacent phenylene rings are all in normal range. Therefore, it suggests that the application of DFT at the B3LYP/6-31G(d) is a good method for reliably optimizing geometry of sulfur-containing imide compound.

The right of Figure 9 shows the charge density isosurfaces of basic unit of APTT-6FDA and 3SDA-6FDA with the most energetically favorable geometry. The relative ordering of the occupied and virtual molecular orbitals gives a reasonable indication of the excited properties and charge transport ability.<sup>35</sup> Both the HOMO and LUMO + 2 isosurface tends to locate on the donor while the LUMO and LUMO + 1 located on the acceptor. The electronic transition corresponds to promotion of an electron at the excited state. This indicates that the electron transfer subsequent to the excitation of the APTT or 3SDA moiety leads to the CT state. The polarized charge transfer mechanism is partially similar to that of TP6F-PI under a condition of applied field.<sup>7</sup> Note that the calculated dipole moment of TP6F-PI is  $2.06$  D, respectively. The theoretical higher dipole moment of APTT-6FDA ( $5.83$  D) and 3SDA-6FDA ( $6.00$  D) compared with TP6F-PI probably leads to a more stable CT complex.<sup>1</sup> Also, the lower HOMO level of 3SDA-6FDA than APTT-6FDA results in to a higher turn-on voltage of the former. Besides, the charges could be segregated and only localized in the donor or acceptor. Therefore, the CT state can be

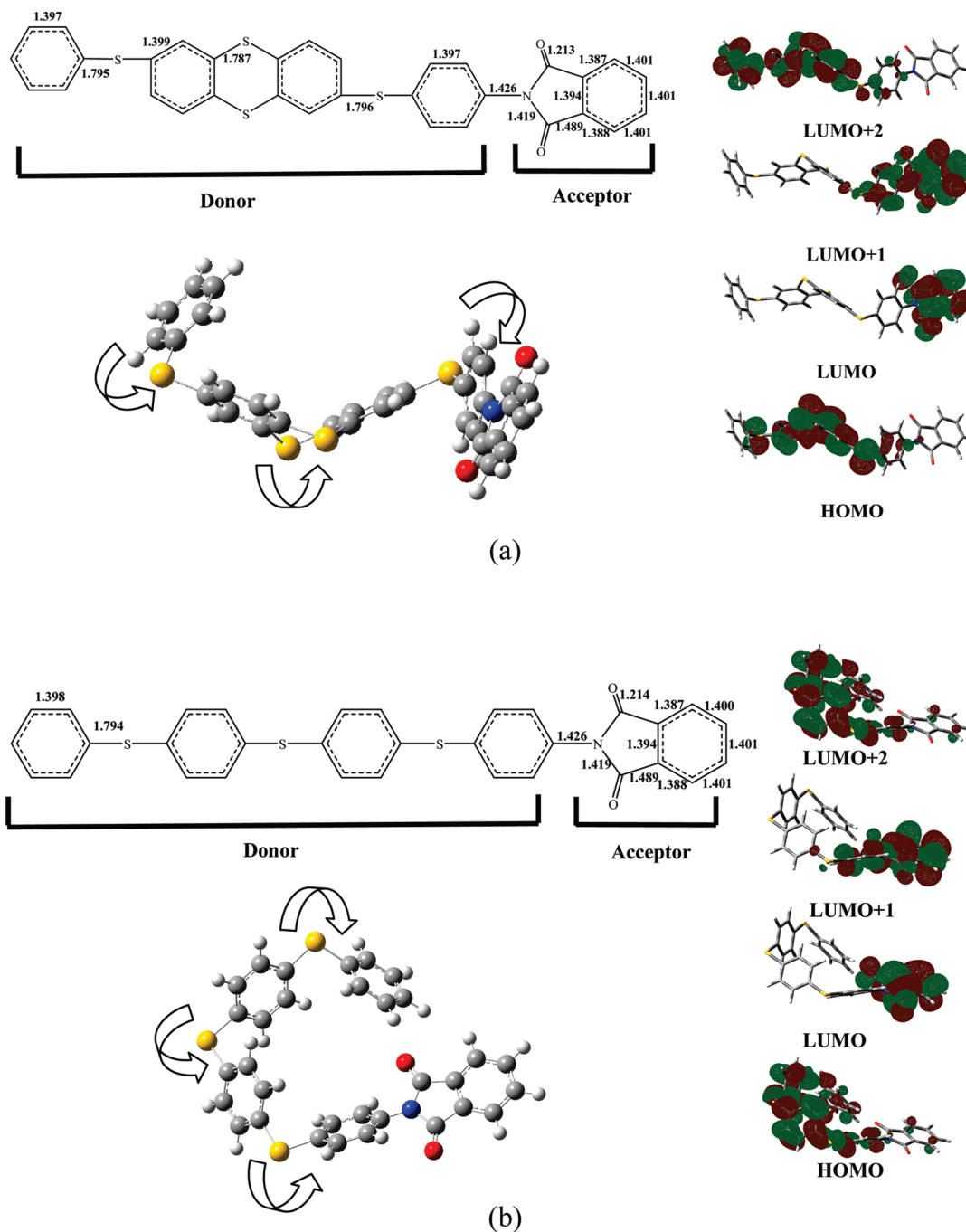


**Figure 9.** Optimized geometries of the basic units and (right) electric density contours for molecular orbitals of the basic units: (a) APTT-6FDA and (b) 3SDA-6FDA.

sustained steadily, and the ON-state remains for a period of time. Only in the negative bias of an electric field can dissociate the CT complex and return to its original OFF-state. Besides, the lower turn-on voltage may also result from the high dipole moment. Also, the high dipole moment of these two sulfur-containing polyimides may play an important role in the enhanced electron-donating and charge-transporting effects. As a result, the memory device of APTT-6FDA and 3SDA-6FDA shows flash memory behavior, and the CT mechanism can also be demonstrated by our theoretical calculation.

## Conclusions

We have successfully synthesized two new sulfur-containing polyimides, APTT-6FDA and 3SDA-6FDA, for the memory

device application. The memory device with the configuration of ITO/polymers/Al showed nonvolatile memory characteristics with the low turn-on threshold voltages around 1.5 and 2.5 V. Also, they could be repeatedly written, read, and erased. The on/off current ratios of the devices were all around  $10^4$  in ambient atmosphere. The different turn-on threshold voltages apparently resulted from the two different low-lying HOMO energy levels. The theoretical analysis suggested that the charge-transfer mechanism could be used to explain the memory characteristics of the studied polyimides. The relatively higher dipole moments of the sulfur-containing polyimides compared to the triphenylamine-based polyimide provided a stable CT complex for the flash memory device. The present study suggests that these new sulfur-containing polyimides have potential applications for memory devices.



**Acknowledgment.** Research work at National Taiwan University is supported by the National Science Council and the Ministry of Economic Affairs of Taiwan.

**Supporting Information Available:**  $^{13}\text{C}$  NMR and DEPT-135 NMR spectra of 3SDA-6FDA; TGA curves of APTT-6FDA and 3SDA-6FDA under a nitrogen or ambient atmosphere; DSC curves of APTT-6FDA and 3SDA-6FDA under a nitrogen atmosphere; configuration of the polymer memory device; AFM surface structures of APTT-6FDA and 3SDA-6FDA memory devices. This material is free of charge via the Internet at <http://pubs.acs.org>.

## References and Notes

- (1) (a) Ling, Q. D.; Liaw, D. J.; Teo, E. Y. H.; Zhu, C.; Chan, D. S. H.; Kang, E. T.; Neoh, K. G. *Polymer* **2007**, *48*, 5182. (b) Ling, Q. D.; Liaw, D. J.; Zhu, C.; Chan, D. S. H.; Kang, E. T.; Neoh, K. G. *Prog. Polym. Sci.* **2008**, *33*, 917.
- (2) Yang, Y.; Ouyang, J.; Ma, L.; Tseng, R. J. H.; Chu, C. W. *Adv. Funct. Mater.* **2006**, *16*, 1001.
- (3) Ling, Q. D.; Knag, E. T.; Neoh, K. G.; Chen, Y.; Zhuang, X. D.; Zhu, C. X.; Chan, D. S. H. *Appl. Phys. Lett.* **2008**, *92*, 143302.
- (4) Kim, T. W.; Oh, S. H.; Choi, H.; Hwang, H.; Kim, D. Y.; Lee, T. *Appl. Phys. Lett.* **2008**, *92*, 253308.
- (5) Majumdar, H. S.; Bolognesi, A.; Pal, A. J. *Synth. Met.* **2004**, *140*, 203.
- (6) Baek, S.; Lee, D.; Kim, J.; Hong, S. H.; Kim, O.; Ree, M. *Adv. Funct. Mater.* **2007**, *17*, 2637.
- (7) Ling, Q. D.; Chang, F. C.; Song, Y.; Zhu, C. X.; Liaw, D. J.; Chan, D. S. H.; Kang, E. T.; Neoh, K. G. *J. Am. Chem. Soc.* **2006**, *128*, 8732.
- (8) Hahm, S. G.; Choi, S.; Hong, S. H.; Lee, T. J.; Park, S.; Kim, D. M.; Kwon, W. S.; Kim, K.; Ree, M. *Adv. Funct. Mater.* **2008**, *18*, 3276.
- (9) Wagn, K. L.; Tseng, T. Y.; Tsai, H. L.; Wu, S. C. *J. Polym. Sci., Part A: Polym. Chem.* **2008**, *46*, 6861.
- (10) Chu, C. W.; Ouyang, J.; Tseng, J. H.; Yang, Y. *Adv. Mater.* **2005**, *17*, 1440.
- (11) Laiho, A.; Majumdar, H. S.; Baral, J. K.; Jansson, F.; Osterbacka, R.; Ikkala, O. *Appl. Phys. Lett.* **2008**, *93*, 203309.
- (12) Huang, C. M.; Liu, Y. S.; Chen, C. C.; Wei, K. H.; Sheu, J. T. *Appl. Phys. Lett.* **2008**, *93*, 203303.
- (13) Leong, W. L.; Lee, P. S.; Lohani, A.; Lam, Y. M.; Chen, T.; Zhang, S.; Dodabalapur, A.; Mhaisakar, S. G. *Adv. Mater.* **2008**, *20*, 2325.
- (14) Kndo, T.; Lee, S. M.; Malicki, M.; Domercq, B.; Marder, S. R.; Kippelen, B. *Adv. Funct. Mater.* **2008**, *18*, 1112.
- (15) Tseng, R. J.; Tsai, C.; Ma, L.; Ouyang, J.; Ozkan, C. S.; Yang, Y. *Nat. Nanotechnol.* **2006**, *1*, 72.
- (16) Choi, T. L.; Lee, K. H.; Joo, W. J.; Lee, S.; Lee, T. W.; Chae, M. Y. *J. Am. Chem. Soc.* **2007**, *129*, 9842.
- (17) Karakawa, M.; Chikamatsu, M.; Yoshida, Y.; Azumi, R.; Yase, K.; Nakamoto, C. *Macromol. Rapid Commun.* **2007**, *28*, 1479.
- (18) Xie, L. H.; Lin, Q. D.; Hou, X. Y.; Huang, W. J. *Am. Chem. Soc.* **2008**, *130*, 2120.
- (19) Lin, J.; Ma, D. *Appl. Phys. Lett.* **2008**, *93*, 093505.
- (20) Janietz, S.; Wedel, A.; Friedrich, R.; Anlauf, S. *Polym. Prepr.* **1999**, *40*, 1219–1220.
- (21) Remonen, T.; Hellberg, J.; von Schutz, J.-U. *Synth. Met.* **1997**, *86*, 1851.
- (22) Morrison, J. J.; Murray, M. M.; Li, X. C.; Holmes, A. B.; Moratti, S. C.; Friend, R. H.; Sirringhaus, H. *Synth. Met.* **1999**, *102*, 987.
- (23) Sakayori, K.; Shibasaki, Y.; Ueda, M. *Polym. J.* **2006**, *28*, 132.
- (24) Liu, J. G.; Nakamura, Y.; Shibasaki, Y.; Ando, S.; Ueda, M. *Macromolecules* **2007**, *40*, 4614.
- (25) Liu, J. G.; Nakamura, Y.; Suzuki, Y.; Shibasaki, Y.; Ando, S.; Ueda, M. *Macromolecules* **2007**, *40*, 7902.
- (26) Liu, J. G.; Nakamura, Y.; Shibasaki, Y.; Ando, S.; Ueda, M. *J. Polym. Sci., Part A: Polym. Chem.* **2007**, *45*, 5606.
- (27) Sun, Q. J.; Wang, H. Q.; Yang, C. H.; Li, Y. F. *J. Mater. Chem.* **2003**, *13*, 800.
- (28) Gaussian 03, Revision B.04: Frisch, M. J.; Trucks, G. W.; Schlegel, H. B.; Scuseria, G. E.; Robb, M. A.; Cheeseman, J. R.; Montgomery, Jr., J. A.; Vreven, T.; Kudin, K. N.; Burant, J. C.; Millam, J. M.; Iyengar, S. S.; Tomasi, J.; Barone, V.; Mennucci, B.; Cossi, M.; Scalmani, G.; Rega, N.; Petersson, G. A.; Nakatsuji, H.; Hada, M.; Ehara, M.; Toyota, K.; Fukuda, R.; Hasegawa, J.; Ishida, M.; Nakajima, T.; Honda, Y.; Kitao, O.; Nakai, H.; Klene, M.; Li, X.; Knox, J. E.; Hratchian, H. P.; Cross, J. B.; Bakken, V.; Adamo, C.; Jaramillo, J.; Gomperts, R.; Stratmann, R. E.; Yazyev, O.; Austin, A. J.; Cammi, R.; Pomelli, C.; Ochterski, J. W.; Ayala, P. Y.; Morokuma, K.; Voth, G. A.; Salvador, P.; Dannenberg, J. J.; Zakrzewski, V. G.; Dapprich, S.; Daniels, A. D.; Strain, M. C.; Farkas, O.; Malick, D. K.; Rabuck, A. D.; Raghavachari, K.; Foresman, J. B.; Ortiz, J. V.; Cui, Q.; Baboul, A. G.; Clifford, S.; Cioslowski, J.; Stefanov, B. B.; Liu, G.; Liashenko, A.; Piskorz, P.; Komaromi, I.; Martin, R. L.; Fox, D. J.; Keith, T.; Al-Laham, M. A.; Peng, C. Y.; Nanayakkara, A.; Challacombe, M.; Gill, P. M. W.; Johnson, B.; Chen, W.; Wong, M. W.; Gonzalez, C.; Pople, J. A. Gaussian, Inc., Wallingford, CT, 2004.
- (29) Hasegawa, M.; Horie, K. *Prog. Polym. Sci.* **2000**, *26*, 259.
- (30) Lim, E. H.; Jung, B. J.; Shim, H. K. *Macromolecules* **2003**, *12*, 4288.
- (31) Tokita, Y.; Ino, Y.; Okamoto, A.; Hasegawa, M.; Shindo, Y.; Sugimura, N. *Jpn. J. Polym. Sci. Technol.* **1994**, *51*, 245.
- (32) Pope, M.; Swenberg, C. E. *Electronic Process in Organic Crystals and Polymers*, 2nd ed.; Oxford University Press: New York, 1999.
- (33) Larson, S. B.; Simonsen, S. H.; Martin, G. E.; Smith, K.; Puig-Torres, S. *Acta Crystallogr.* **1984**, *C40*, 103.
- (34) Li, R. *Acta Crystallogr.* **2006**, *E62*, 5600.
- (35) Marcos, A. D. O.; Duarte, H. A.; Pernaut, J. M.; Wagner, B. D. A. *J. Phys. Chem. A* **2000**, *104*, 143302.